JOURNAL OF MATERIALS SCIENCE 15 (1980) 3071–3080

On elastic incompatibility during the deformation of α – β brass two-phase bicrystals

NABIL FAT-HALLA*
Graduate School, Tohoku University, Sendai, Japan
TAKAYUKI TAKASUGI, OSAMU IZUMI
Research Institute for Iron, Steel and Other Metals, Tohoku University, Sendai, Japan

The effect of the elastic incompatibility on the deformation of α–β brass two-phase bicrystals was studied at temperatures of 150, 300 and 450 K. At 150 and 300 K, the curvature of the slip traces in the β-component with distance from the interface was found to be closely related to the exponential decay of the elastic incompatible stresses with distance from the interface. More than four slip systems (which are necessary for the plastic compatibility theory) were observed to operate and although the total number of slip systems differed from one specimen to another, it can be rigidly concluded that additional slip systems have been activated due to the elastic compatibility requirements.

1. Introduction

The deformation behaviours of one- [1–7] and two-phase [8–15] bicrystals have been extensively studied during the last few years. These previous investigations have, undoubtedly, put forward the interpretation of the deformation behaviours of polycrystals in connection with those of single crystals. Some attention has already been given to the effect of the elastic incompatibility on the deformation of one-phase bicrystals [3–7]. However, in the case of two-phase bicrystals, the effect of elastic incompatibility on deformation behaviour is expected to be much more remarkable since the interface in this case separates two different crystal structures.

The deformation of the α–β brass two-phase bicrystals has been recently reported by the present authors [9–15], however, emphasis was mainly given to the effect of plastic incompatibility on deformation behaviour. The purpose of the present study is to clarify the elastic incompatibility effect on the deformation at three test temperatures (150, 300 and 450 K). These temperatures were selected since the deformation characteristics of the constituents are known to change distinctly at these temperatures [16–21]. Temperatures lower than 150 K were not selected so that the occurrence of the martensitic transformation in the β-component could be avoided [22]; tests at temperatures higher than 450 K were not conducted in order to avoid the problem of decomposition.

2. Experimental procedure

The α–β brass two-phase bicrystals were prepared following the same procedure as that mentioned in a previous work [9]. These bicrystals showed flat interfaces and almost constant zinc concentration profiles in both phases [9]. The orientation relationship between the two constituents implied the matching of the close packed planes $\{1\,1\,1\}_\alpha$ and $\{1\,1\,0\}_\beta$ [9] with some scattering.

Tensile specimens were prepared using a spark cutting machine with the gauge dimensions 2 mm × 3 mm × 18 mm (see Fig. 1). The tensile tests were conducted in an alcohol medium at 150 K, in air at room-temperature and in a silicon oil bath at 450 K. The slip traces at about 3%

*Present address: Mechanical Engineering Department, Al-Azhar University, Cairo, Egypt.

0022–2461/80/123071–10$03.00/0

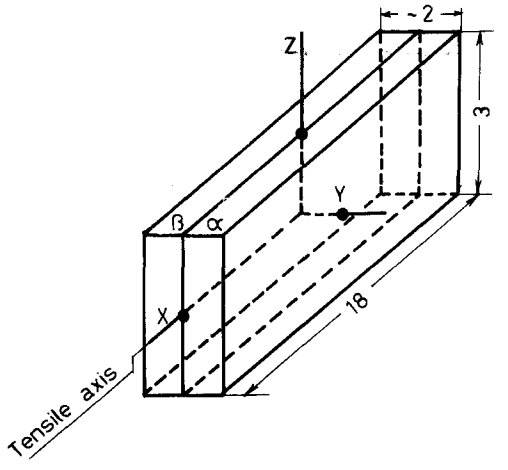

Figure 1 Bicrystal geometry and gauge dimensions (in mm).

plastic strain were observed by optical microscopy. The operative slip systems were determined on stereographic projections determined by the usual X-ray back reflection Laue method.

3. Theoretical discussion

Elastic incompatibility will, in general, exist. Firstly, during the deformation of an isoaxial bicrystal [1–7] when it is subjected to a uniaxial stress σ_x (see Fig. 1) in the elastic range, and one of the compatibility relations* is satisfied ($\epsilon_x^\alpha = \epsilon_x^\beta$) and the remaining two are not likely to be satisfied. Secondly, when a non-isoaxial bicrystal [1–7] is deformed under a condition of uniform axial elastic strain, then the component crystals are not equally stressed, resulting in elastic incompatibilities at the interface. The ratio of the applied stresses is proportional to the ratio of the elastic moduli of the two component crystals in the axial direction [4],

$$\frac{\sigma_x^\alpha}{\sigma_x^\beta} = \frac{E_x^\alpha}{E_x^\beta}, \tag{1}$$

where E_x^α and E_x^β are the Young's moduli for the α- and β-components in the axial direction, respectively. The ratio $(\sigma_x^\alpha/\sigma_x^\beta)$ depends only on the relative moduli of the components and is independent of their relative cross-sectional areas. The component crystal having a high modulus will be stressed to a higher level than the component with low modulus at the same level of total load. For the present bicrystal, where the volume fractions of the α- and β-components were nearly the same, the total stress, σ_T, on the bicrystal in the x-direction is related to the stress on the α-component, σ_x^α, by the following equation:

$$\sigma_T = \frac{\sigma_x^\alpha}{2}\left(1 + \frac{E_x^\beta}{E_x^\alpha}\right), \tag{2}$$

where E_x^α and E_x^β are the elastic stiffnesses of the α- and β-components in the x-direction. If the Schmid factor, m, and the critical resolved shear stress (CRSS) are known for the α-component (the softer component) then it is possible, through the aid of Equation 2, to obtain value for σ_T at the end of the elastic stage (i.e. at the onset of plastic yielding in the α-component).

The estimation of the elastic incompatibility at the interface of a bicrystal necessitates the calculation of the elastic strain components in the x-, z- and xz- directions (see Fig. 1). These elastic strain components can be calculated using the following equations [23]:

$$\epsilon_{ij} = \frac{1}{E}\cdot\sigma = \{S_{11} - 2[(S_{11} - S_{12}) - \tfrac{1}{2}S_{44}](l^2m^2 + m^2n^2 + n^2l^2)\}\sigma, \tag{3}$$

$$\gamma_{ij} = \frac{1}{G}\cdot\tau = \{S_{44} - 2[(S_{11} - S_{12}) - \tfrac{1}{2}S_{44}](l^2m^2 + m^2n^2 + n^2l^2)\}\tau, \tag{4}$$

where S_{ij} represents the standard compliances of the component crystals and l, m and n are the direction cosines of the specified direction with respect to that of the crystallographic axes. Since the main purpose of the present investigation was to study the effect of the elastic incompatibility on the deformation behaviours of the α–β brass two-phase bicrystals, it is significant to review the values of the elastic constants (stiffnesses, C_{ij}, and compliances, S_{ij}) for the component-phases at the three test temperatures under consideration. The standard compliances were obtained from the standard stiffnesses through the following relations [24]:

$$S_{44} = \frac{1}{C_{44}}, \tag{5}$$

$$S_{11} = \frac{C_{11} + C_{12}}{(C_{11} - C_{12})(C_{11} + 2C_{12})}, \tag{6}$$

$$S_{12} = \frac{-C_{12}}{(C_{11} - C_{12})(C_{11} + 2C_{12})}. \tag{7}$$

*The compatibility relations at the interface of a bicrystal are: $\epsilon_x^\alpha = \epsilon_x^\beta$; $\epsilon_z^\alpha = \epsilon_z^\beta$; $\gamma_{xz}^\alpha = \gamma_{xz}^\beta$.

TABLE I Elastic standard stiffnesses, C_{ij} and compliances, S_{ij} for the α- and β-brass single-crystals

Component	Temperature (K)	C_{11} ($\times 10^9$ N m^{-2})	C_{12} ($\times 10^9$ N m^{-2})	C_{44} ($\times 10^9$ N m^{-2})	S_{11} ($\times 10^{-12}$ m^2 N^{-1})	S_{12} ($\times 10^{-12}$ m^2 N^{-1})	S_{44} ($\times 10^{-12}$ m^2 N^{-1})
	150	152	112	75	17.5	−7.4	13.3
α	300	146	111	72	19.4	−8.4	13.9
	450	139	107	67	21.8	−9.5	14.9
	150	139	121	87	37.9	−17.9	11.5
β	300	130	114	79	42.5	−20	12.7
	450	128	113	74	45.6	−21.4	13.5

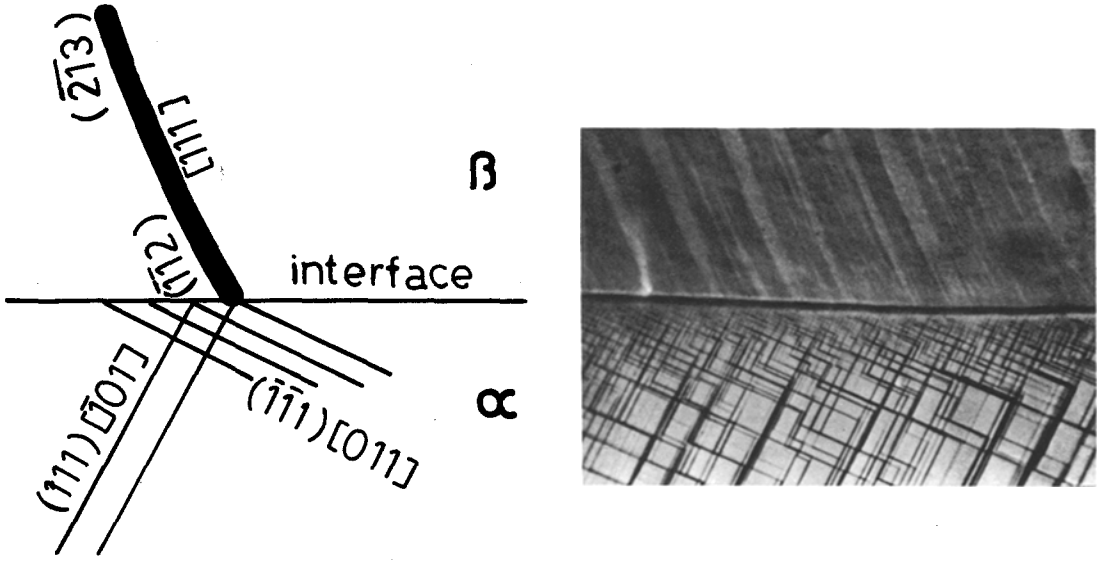

Figure 2 Slip traces observed on the narrow face of a typical α–β brass bicrystal at 150 K (3% plastic strain).

Table I lists the elastic constants for the α-component [25] and β-component [26] phases* as a basis for later discussions.

4. Results and discussion

The results will now be presented and discussed for each test temperature.

4.1. Study conducted at 150 K

Fig. 2 shows the slip traces, at 3% plastic strain, as observed on the narrow face (parallel to the xy plane in Fig. 1) perpendicular to the interface, at 150 K. The slip traces on the α-component were well-defined, straight and band-like and they always corresponded to the type $\{1\,1\,1\}_\alpha\langle 1\,1\,0\rangle_\alpha$. Two slip systems can be clearly observed on the α-component being the primary $(1\,1\,1)_\alpha[\bar{1}\,0\,1]_\alpha$ and the conjugate $(\bar{1}\,\bar{1}\,1)_\alpha[0\,1\,1]_\alpha$. The latter system, $(\bar{1}\,\bar{1}\,1)_\alpha[0\,1\,1]_\alpha$, is believed to be activated by the elastic incompatibility effect since the slip intensity was higher near the interface and decreased with distance away from it (this should be related to the exponential decay of the elastic incompatible stresses with distance from the interface [7]). The slip traces on the β-component were seen as broad-bands curved with distance from the interface. The slip direction always corresponded to the $[1\,1\,1]_\beta$ but the slip plane changed continuously from $(\bar{1}\,\bar{1}\,2)_\beta$ at the interface to $(\bar{2}\,\bar{1}\,3)$ in the interior of the β-matrix.

Generally, it is believed that the operative slip systems in the bicrystals considered here are controlled by three factors: (1) the Schmid factors of both component crystals, (2) the N_{ij}† value and (3) the elastic incompatibility. These factors will be analysed in the following discussion.

Table II lists the Schmid factor, m, for various slip systems in the α- and β-components. The N_{ij} [1] values are listed in Table III. The elastic compliances in the x-, z- and xz-directions are documented in Table IV. Now it is easy to calculate the plastic-strain [1–7] and elastic-strain components in the x-, z- and xz-directions at the interface. These values are documented in Table V. If the elastic stresses are now resolved (as represented by the elastic strains in Table V) on the slip systems of importance in both phases through n and l resolving factors (analogous to the Schmid factor) then the intensity of the elastically induced stresses on each slip system can be estimated. Taking into account that n is the resolving factor for τ_{xz} and l is the resolving factor for σ_z, Tables VI and VII were thus obtained.

Referring to Table II it can be noted that the $(1\,1\,1)_\alpha[\bar{1}\,0\,1]_\alpha$ system possesses the highest m value ($m = 0.5$) and, thus, the highest resolved

*Some of the constants needed for temperatures or compositions used in the present work were obtained by extrapolation from [25, 26].

†The N_{ij} factor [1] is one controlling the activation of slip in one component by the stress concentration induced by slip on the other component.

TABLE II The Schmid factors for the possible slip systems measured at a temperature of 150 K

α-component					
Slip systems	$(11\bar{1})[\bar{1}01]$*	$(\bar{1}11)[101]$	$(\bar{1}\bar{1}1)[011]$†	$(1\,\bar{1}\,1)[\bar{1}\,0\,1]$‡	$(111)[\bar{1}10]$
Schmid factors	0.50	0.46	0.38	0.27	0.23
β-component					
Slip systems	$(\bar{1}01)[111]$	$(101)[\bar{1}11]$†	$(1\,\bar{1}\,0)[1\,1\,1]$‡	$(\bar{2}\bar{1}3)[111]$*	$\rightarrow(\bar{1}\bar{1}2)[111]$*
Schmid factors	0.49	0.46	0.23	0.47	0.43

*Primary slip system. In the case of the β-component crystal the arrow head indicates the slip plane in the interior while the other end of the arrow indicates the slip plane at the interface.
†Conjugate slip system.
‡Matching planes.

TABLE III The N_{ij} values for different combinations of slip systems measured at a temperature of 150 K

α- and β-slip systems	N_{ij}
$(111)_\alpha[\bar{1}01]_\alpha \cdot (\bar{1}01)_\beta[111]_\beta$	0.96
$(111)_\alpha[\bar{1}01]_\alpha \cdot (\bar{2}13)_\beta[111]_\beta$	0.81
$(111)_\alpha[\bar{1}01]_\alpha \cdot (\bar{1}\bar{1}2)_\beta[111]_\beta$	0.68
$(111)_\alpha[\bar{1}01]_\alpha \cdot (101)_\beta[\bar{1}11]_\beta$	0.81
$(111)_\alpha[\bar{1}01]_\alpha \cdot (1\bar{1}0)_\beta[111]_\beta$	0.72
$(\bar{1}11)_\alpha[101]_\alpha \cdot (\bar{1}\bar{1}2)_\beta[111]_\beta$	0.81
$(\bar{1}\bar{1}1)_\alpha[011]_\alpha \cdot (\bar{1}\bar{1}2)_\beta[111]_\beta$	0.32
$(1\bar{1}1)_\alpha[\bar{1}01]_\alpha \cdot (\bar{1}\bar{1}2)_\beta[111]_\beta$	0.88
$(111)_\alpha[\bar{1}10]_\alpha \cdot (\bar{1}\bar{1}2)_\beta[111]_\beta$	0.34
$(1\bar{1}1)_\alpha[\bar{1}01]_\alpha \cdot (1\bar{1}0)_\beta[111]_\beta$	1.00§

§This combination contains the matching planes.

shear stress. Consequently it was observed to operate as a primary slip system in the α-component. Now, with reference only to Tables II and III, it can be seen that the $(\bar{1}\,0\,1)_\beta[1\,1\,1]_\beta$ system in the β-component is the most highly stressed and therefore, the most favourable component to operate as a primary slip system. However, the system that was activated at the interface is near to $(\bar{1}\,\bar{1}\,2)_\beta[1\,1\,1]_\beta$. To have a clear interpretation of this result two factors must be taken into consideration: the first being that the CRSS towards $\{1\,1\,2\}_\beta\langle 1\,1\,1\rangle_\beta$ is lower than that for the $\{1\,1\,0\}_\beta\langle 1\,1\,1\rangle_\beta$ at the present test temperature for the β-component and the second being the values of the resolved shear stress (RSS) due to the elastic incompatibility on the slip systems under consideration. The first factor is known to result in the operation of a slip system having a plane with a high index lying between the $(\bar{1}\,0\,1)_\beta$ and $(\bar{1}\,\bar{1}\,2)_\beta$ planes or coinciding with the latter, depending on the test temperature [18] and the orientation of the specimen [19]. If the second factor is now taken into consideration, it can be noted from Table IV that this bicrystal is elastically incompatible and from Table V that the elastic incompatibility in the xz-direction is more severe (a higher value) than that in the z-direction. Thus, it is expected that the former would have a more significant role on the activation of the slip systems. With the aid of Table VI it can be seen that the elastically induced RSS on the $(\bar{1}\,\bar{1}\,2)_\beta$ $[1\,1\,1]_\beta$ system with respect to the xz-direction is

TABLE IV The elastic compliances at the interface measured at a temperature of 150 K

Components	S_{xx} ($\times 10^{-12}$ m^2 N^{-1})	S_{zz} ($\times 10^{-12}$ m^2 N^{-1})	S_{xz} ($\times 10^{-12}$ m^2 N^{-1})
α-crystal	+ 9.83	− 17.50	+ 11.11
β-crystal	+ 20.00	− 15.01	− 23.32

TABLE V The plastic and elastic strain components at the interface measured at a temperature of 150 K

Strain components	α-component			β-component	
	Plastic		Elastic ($\times 10^{-12}$)	Plastic	Elastic ($\times 10^{-12}$)
	$(111)[\bar{1}01]$	$(\bar{1}\bar{1}1)[011]$		$(\bar{1}\bar{1}2)[111]$	
ϵ_{xx}	$0.52s_1^\alpha$	$0.39s_2^\alpha$	$+ 9.33\sigma_x^\alpha$	$+ 0.39s_1^\beta$	$+ 9.83\sigma_x^\alpha$
ϵ_{zz}	$0.38s_1^\alpha$	$0.06s_2^\alpha$	$- 17.50\sigma_x^\alpha$	$+ 0.49s_1^\beta$	$- 7.38\sigma_x^\alpha$
γ_{xz}	$0.03s_1^\alpha$	$- 0.22s_2^\alpha$	$+ 11.11\sigma_x^\alpha$	$- 0.11s_1^\beta$	$- 11.46\sigma_x^\alpha$

TABLE VI The resolving factors n and l for the elastic stresses in β measured at a temperature of 150 K

Factor	System				
	$(\bar{1}01)[111]$	$(2\bar{1}3)[111]$	$(\bar{1}\bar{1}2)[111]$	$(101[\bar{1}11]$	$(1\bar{1}0)[111]$
n	0.02	0.03	0.07	0.34	0.16
l	0.48	0.51	0.50	0.12	0.11

TABLE VII The resolving factors n and l for the elastic stresses in α measured at a temperature of 150 K

Factor	System			
	$(\bar{1}\bar{1}1)[011]$	$(\bar{1}11)[101]$	$(1\bar{1}1)[\bar{1}01]$	$(111)[\bar{1}10]$
n	0.33	0.10	0.13	0.29
l	0.06	0.32	0.13	0.28

higher than that for the $(\bar{2}\,\bar{1}\,3)_\beta[1\,1\,1]_\beta$ system, and that the elastically induced RSS in the z-direction is nearly equal for the two systems. Therefore, it can be concluded that the system $(\bar{1}\,\bar{1}\,2)_\beta[1\,1\,1]_\beta$ observed at the interface is favoured elastically while the $(\bar{2}\,\bar{1}\,3)_\beta[1\,1\,1]_\beta$ system was concluded to operate in the interior of the β-matrix, reflecting the higher m and N_{ij} values for the latter system. The curvature of the slip traces on the β-component can thus be interpreted as resulting from the change of the incompatible elastic stresses with distance from the interface. Now, if the conjugate slip system in the α-component is guessed, referring to Tables II and III only, the system $(\bar{1}\,1\,1)_\alpha[1\,0\,1]_\alpha$ might be operated. However, the actually observed slip system was the conjugate slip system $(\bar{1}\,\bar{1}\,1)_\alpha$ $[1\,0\,1]_\alpha$. Again, this result can be explained on the basis of the elastic incompatible stresses. Referring to Table VII it can be noted that the n value for the $(\bar{1}\,\bar{1}\,1)_\alpha[0\,1\,1]_\alpha$ system is comparatively higher than that for the $(\bar{1}\,1\,1)_\alpha[1\,0\,1]_\alpha$ system (the latter having higher values of m and N_{ij}). Although the l value for the latter system is higher, the decisive value is that of n (compare with Table V) since the elastic incompatibility in the xz-direction is higher than that in the z-direction. Therefore, taking the elastic incompatibility into consideration, the $(\bar{1}\,\bar{1}\,1)_\alpha[0\,1\,1]_\alpha$ system was the most favourable being consistent with the experimentally observed one. Thus, the elastic incompatible stresses have a significant effect on the deformation characteristics of the present bicrystals, i.e. slip systems not expected from the plastic deformation of the bicrystals were observed to operate due to the consideration of the elastic incompatibility.

4.2. Study conducted at 300 K

Fig. 3 shows the slip traces observed at 300 K for 3% plastic strain. At the present temperature the β-traces were fine and ill-defined instead of being seen as broad bands as at 150 K. Since this change in slip trace characteristics refers to the

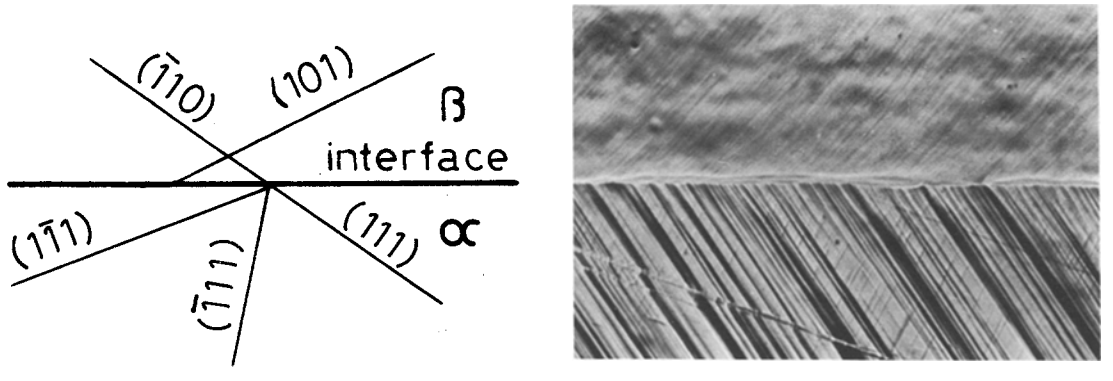

Figure 3 Slip traces observed on the narrow face of a typical α–β brass bicrystal tested at room-temperature. (3% plastic strain).

TABLE VIII The Schmid factors for the possible slip systems measured at a temperature of 300 K

α-component					
Slip systems	$(111)_\alpha[\bar{1}01]_\alpha$*†	$(\bar{1}\bar{1}1)_\alpha[011]_\alpha$†	$(\bar{1}\bar{1}1)_\alpha[011]_\alpha$	$(1\bar{1}1)_\alpha[011]_\alpha$	$(1\bar{1}1)_\alpha[\bar{1}01]_\alpha$
Schmid factors	0.35	0.32	0.18	0.15	0.14
β-component					
Slip systems	$(\bar{1}01)_\beta[111]_\beta$	$(\bar{2}11)_\beta[111]_\beta$	$(\bar{3}12)_\beta[111]_\beta$	$(101)_\beta[\bar{1}11]_\beta$	$(\bar{1}\bar{1}0)_\beta[\bar{1}11]_\beta$††
Schmid factors	0.43	0.47	0.47	0.38	0.35

*Primary system
†Conjugate system
††Matching planes.

behaviour of the β-brass single crystal at the two test temperatures it need not be discussed here. The observed slip systems in the α-component corresponded always to the type $\{1\,1\,1\}_\alpha\langle 1\,1\,0\rangle_\alpha$ while those in the β-component changed continuously from around $(\bar{1}\,0\,1)_\beta$ at the interface to a plane of higher index between $(\bar{3}\,1\,2)_\beta$ and $(\bar{2}\,1\,1)_\beta$ in the interior of the β-component.

These results are also believed to relate to the elastic incompatible stresses and will be analysed in Tables VIII–XI.

In this bicrystal, although the Schmid factor m is larger in β than in α for the primary slip systems (see Table VIII), it is expected that the α-component would deform plastically before the β-component owing to the high value of the ratio $\sigma_x^\alpha/\sigma_x^\beta$ (~ 2) and due to the relatively lower CRSS for the α-component. The system $(1\,1\,1)_\alpha[\bar{1}\,0\,1]_\alpha$ was thus observed to operate primarily in α. If the m and N_{ij} values, given in Tables VIII and IX, respectively, are now taken into consideration, it can be seen that, for the β-components, the systems $(\bar{2}\,1\,1)_\beta[1\,1\,1]_\beta$ and $(\bar{3}\,1\,2)_\beta[1\,1\,1]_\beta$, respectively, are the most favourable. However, the system that was experimentally observed at the interface was the $(\bar{1}\,0\,1)_\beta[1\,1\,1]_\beta$. This result definitely indicates that some factor other than the m and N_{ij} values was responsible for the activation of this system. Therefore, this third factor must be the elastic incompatible stresses. As can be seen from Table X the bicrystal used here is elastically incompatible and, therefore, it is expected that the activated slip system near the interface being around $(\bar{1}\,0\,1)_\beta[1\,1\,1]_\beta$ was the system having the highest total resolved shear stress (TRSS), depending not only on the m and N_{ij} values but also on the resolved shear stress (RSS) due to the elastic incompatible stresses.

TABLE IX The N_{ij} values for different combinations of slip systems measured at a temperature of 300 K

α- and β-slip systems	N_{ij}
$(111)_\alpha[\bar{1}01]_\alpha \cdot (\bar{1}01)_\beta[111]_\beta$	0.68
$(111)_\alpha[\bar{1}01]_\alpha \cdot (\bar{3}12)_\beta[111]_\beta$	0.86
$(111)_\alpha[\bar{1}01]_\alpha \cdot (\bar{2}11)_\beta[111]_\beta$	0.94
$(\bar{1}\bar{1}1)_\alpha[011]_\alpha \cdot (\bar{3}12)_\beta[111]_\beta$	0.86
$(111)_\alpha[\bar{1}01]_\alpha \cdot (\bar{1}10)_\beta[111]_\beta$	0.98
$(111)_\alpha[\bar{1}01]_\alpha \cdot (101)_\beta[\bar{1}11]_\beta$	0.81
$(\bar{1}\bar{1}1)_\alpha[011]_\alpha \cdot (\bar{2}11)_\beta[111]_\beta$	0.83
$(\bar{1}\bar{1}1)_\alpha[011]_\alpha \cdot (\bar{1}\bar{1}0)_\beta[\bar{1}11]_\beta$*	1.00

*This combination includes the matching planes.

TABLE X The elastic compliances at the interface measured at a temperature of 300 K

Components	S_{xx} ($\times 10^{-12}$ m^2 N^{-1})	S_{zz} ($\times 10^{-12}$ m^2 N^{-1})	S_{xz} ($\times 10^{-12}$ m^2 N^{-1})
α-crystal	+ 6.92	− 13.58	+ 3.92
β-crystal	+ 13.82	− 18.23	− 21.49

TABLE XI The plastic and elastic strain components at the interface measured at a temperature of 300 K

Strain components	α-component			β-component	
	Plastic		Elastic ($\times 10^{-12}$)	Plastic	Elastic ($\times 10^{-12}$)
	$(111)_\alpha[\bar{1}01]_\alpha$	$(\bar{1}\bar{1}1)_\alpha[011]_\alpha$		$(\bar{1}01)_\beta[111]_\beta$	
ϵ_{xx}	$0.35s_1^\alpha$	$0.34s_2^\alpha$	$+ 6.92\sigma_x^\alpha$	$0.44s_1^\beta$	$+ 6.92\sigma_x^\alpha$
ϵ_{zz}	$0.24s_1^\alpha$	$0.16s_2^\alpha$	$- 13.58\sigma_x^\alpha$	$0.17s_1^\beta$	$- 9.22\sigma_x^\alpha$
γ_{xz}	$- 0.31s_1^\alpha$	$0.06s_2^\alpha$	$+ 3.92\sigma_x^\alpha$	$0.06s_1^\beta$	$- 10.76\sigma_x^\alpha$

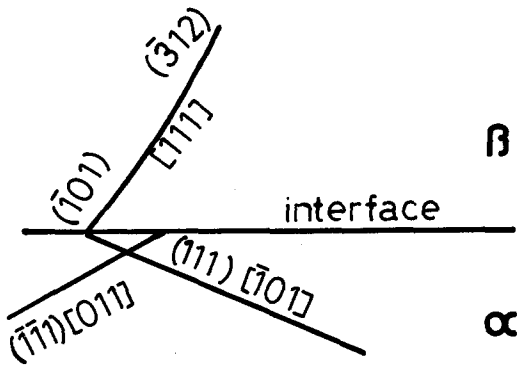

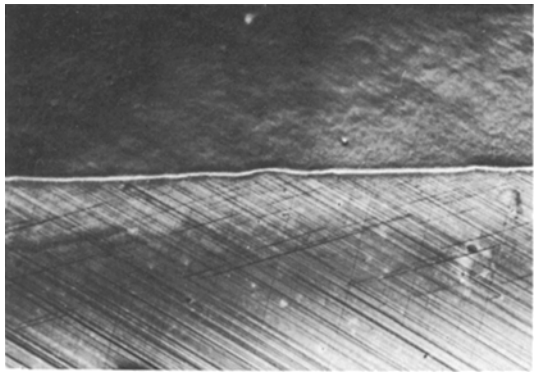

Figure 4 Slip traces observed on a typical α–β brass bicrystal tested at 450 K (3% plastic strain).

TABLE XII Schmid factors for the possible slip systems measured at a temperature of 450 K

α-components					
Slip systems	$(111)_\alpha[\bar{1}01]_\alpha$ p*	$(\bar{1}\bar{1}1)_\alpha[011]_\alpha$	$(1\bar{1}1)_\alpha[\bar{1}01]_\alpha$	$(1\bar{1}1)_\alpha[011]_\alpha$ s	$(\bar{1}11)_\alpha[101]_\alpha$ c
Schmid factors	0.39	0.25	0.13	0.16	0.22
β-components					
Slip systems	$(\bar{1}01)_\beta[111]_\beta$	$(101)_\beta[\bar{1}11]_\beta$ p	$(\bar{1}10)_\beta[111]_\beta$ c*	$(\bar{1}\bar{1}2)_\beta[111]_\beta$	$(\bar{2}11)_\beta[111]_\beta$
Schmid factors	0.44	0.43	0.39	0.27	0.48

p: primary slip system
c: conjugate slip system
s: secondary slip system
* matching planes.

Thus, the observed curved slip traces in β (see Fig. 3) support the above mentioned criterion since it indicates a change in the slip plane corresponding to the change of the TRSS plane.

4.3. Study conducted at 450 K

Fig. 4 shows the slip traces observed on the narrow face perpendicular to the interface plane of the bicrystal tested in tension at 450 K up to 3% plastic strain. The slip traces were straight and well-defined on both components. Three slip systems could be observed to operate in the α-component while two could be observed in the β-component. In the α-component the primary $(1\,1\,1)_\alpha[\bar{1}\,0\,1]_\alpha$ and the conjugate $(\bar{1}\,1\,1)_\alpha$ $[1\,0\,1]_\alpha$ in addition to the secondary $(1\,\bar{1}\,1)_\alpha$ $[0\,1\,1]_\alpha$ were observed to operate. The secondary slip traces did not extend to the wide face parallel to the interface. On the other hand, the β-component exhibited a primary slip system $(1\,0\,1)_\beta[\bar{1}\,1\,1]_\beta$ and the slip system $(\bar{1}\,1\,0)_\beta$ $[1\,1\,1]_\beta$. The latter system includes the matching plane. These results will be clarified in Tables XII to XVII.

TABLE XIII The N_{ij} values for different combinations of slip systems measured at a temperature of 450 K

α-slip system β-slip system	N_{ij}
$(111)_\alpha[\bar{1}01]_\alpha \cdot (\bar{1}01)_\beta[111]_\beta$	0.50
$(111)_\alpha[\bar{1}01]_\alpha \cdot (101)_\beta[\bar{1}11]_\beta$	0.86
$(111)_\alpha[\bar{1}01]_\alpha \cdot (\bar{1}10)_\beta[111]_\beta$	1.00*
$(\bar{1}\bar{1}1)_\alpha[101]_\alpha \cdot (101)_\beta[\bar{1}11]_\beta$	0.74
$(1\bar{1}1)_\alpha[011]_\alpha \cdot (101)_\beta[\bar{1}11]_\beta$	0.63
$(1\bar{1}1)_\alpha[011]_\alpha \cdot (101)_\beta[\bar{1}11]_\beta$	0.51

*This combination contains the matching planes.

The straight slip traces observed on the surface of the β-component when the bicrystal is tested at 450 K is believed to be related to the restricted slip on the $\{1\,1\,0\}_\beta\langle 1\,1\,1\rangle_\beta$ system at the present test temperature [19, 21]. Therefore, in contrast to the results obtained at temperatures of 150 and 300 K, in which the compatibility requirements caused curved slip traces in the β-component, at 450 K these requirements could result in the activation of new slip systems having rather straight traces on the $\{1\,1\,0\}_\beta\langle 1\,1\,1\rangle_\beta$ type of slip systems.

Now, referring to Table XII, it can be noted that the primary slip system in the α-component corresponded to the $(1\,1\,1)_\alpha[\bar{1}\,0\,1]_\alpha$ system ($m = 0.39$ which is the highest value). The primary $(1\,1\,1)_\alpha$ $[\bar{1}\,0\,1]_\alpha$ being operated exerts a shear stress on

TABLE XIV The elastic compliances at the interface measured at a temperature of 450 K

Component	S_{xx} ($\times 10^{-12}$ m^2 N^{-1})	S_{zz} ($\times 10^{-12}$ m^2 N^{-1})	S_{xz} ($\times 10^{-12}$ m^2 N^{-1})
α-crystal	+ 0.3	− 12.3	+ 14.6
β-crystal	+ 16.7	− 12.6	− 29.3

TABLE XV The plastic and elastic strain components at the interface measured at a temperature of 450 K

Strain component	α-component			β-component	
	Plastic		Elastic ($\times 10^{-12}$)	Plastic	Elastic ($\times 10^{-12}$)
	$(111)_\alpha[\bar{1}01]_\alpha$	$(\bar{1}11)_\alpha[101]_\alpha$		$(101)_\beta[\bar{1}11]_\beta$	
ϵ_{xx}	$0.39s_1^\alpha$	$0.17s_2^\alpha$	$+ 0.3\sigma_x^\alpha$	$0.38s_1^\beta$	$+ 0.3\sigma_x^\alpha$
ϵ_{zz}	$0.11s_1^\alpha$	$0.01s_2^\alpha$	$- 12.3\sigma_x^\alpha$	$0.10s_1^\beta$	$- 0.2\sigma_x^\alpha$
γ_{xz}	$0.05s_1^\alpha$	$0.15s_2^\alpha$	$+ 14.6\sigma_x^\alpha$	$- 0.01s_1^\beta$	$- 0.5\sigma_x^\alpha$

the various slip systems of the β-component, the magnitude of which is proportional to the N_{ij} values listed in Table XIII. Taking the three factors of importance being the Schmid factor m, the N_{ij} values and lastly the elastic incompatibility into consideration the slip systems to be operated in the β-component can be predicted. It can be noted that two systems, being the $(1\,0\,1)_\beta[\bar{1}\,1\,1]_\beta$ and the $(\bar{1}\,1\,0)_\beta[1\,1\,1]_\beta$, are to be compromised. Referring to Tables XII, XIII and XVI, it can be observed that while the m value is higher for the former system by about 10%, the N_{ij} value is higher for the latter system by about 16% and that the n and l values are exactly the same. These two systems were observed to operate. The operation of the slip systems in the β-component exerts a shear stress on the slip systems in the α-component which resulted in the operation of the conjugate slip system $(\bar{1}\,1\,1)_\alpha[1\,0\,1]_\alpha$ which has relatively low m value. The operation of the secondary slip system $(1\,\bar{1}\,1)_\alpha[0\,1\,1]_\alpha$ can be interpreted owing to the highest value of the elastically resolved shear stress (compare with the n and l values given in Table XVII). This criterion is strongly supported by the experimental evidence that this system did not extend to the wide face, indicating the decay of the elastic stresses with distance from the interface. Finally, it should be emphasized that slip systems having Schmid factors as low as 0.16 were observed to operate (see Table XII), which reflect the high values of the incompatible stresses under the present test conditions.

TABLE XVI Resolving factors n and l for the elastic stresses in β measured at a temperature of 450 K

Factor	System		
	$(\bar{1}01)_\beta[111]_\beta$	$(101)_\beta[\bar{1}11]_\beta$	$(\bar{1}10)_\beta[111]_\beta$
n	0.03	0.34	0.34
l	0.37	0.09	0.09

5. Conclusions

The elastic incompatibility was found to play a remarkable role on the deformation of the α–β brass two-phase bicrystals at temperatures of 150, 300 and 450 K. In the β-component at 150 and 300 K the curvature of the slip traces with distance from the interface was found to be closely related to the elastic incompatible stresses and its well-known decay with distance from the interface. At 450 K, more than four slip systems were observed to operate in the bicrystal, there being three in the α-component and two in the β-component, thus indicating the effect of the elastic incompatibility since the most incompatible bicrystal would deform on only a total of four slip systems when only the plastic incompatibility is taken into consideration.

TABLE XVII Resolving factors n and l for the elastic stresses in α measured at a temperature of 450 K

Factor	System			
	$(111)_\alpha[\bar{1}01]_\alpha$	$(\bar{1}\bar{1}1)_\alpha[0\bar{1}1]_\alpha$	$(1\bar{1}1)_\alpha[011]_\alpha$	$(\bar{1}\bar{1}1)_\alpha[0\bar{1}1$
n	0.29	0.13	0.27	0.04
l	0.11	0.12	0.10	0.04

References

1. J. D. LIVINGSTON and B. CHALMERS, *Acta Metall.* **5** (1957) 322.
2. J. J. HAUSER and B. CHALMERS, *ibid.* **9** (1961) 802.
3. R. E. HOOK and J. P. HIRTH, *ibid.* **15** (1967) 535.
4. *Idem, ibid.* **15** (1967) 1099.
5. Y. CHUANG and H. MARGOLIN, *Met. Trans.* **4** (1973) 1905.
6. T. D. LEE and H. MARGOLIN, *ibid.* **8A** (1977) 157.
7. J. P. HIRTH, *ibid.* **3** (1972) 3047.
8. K. A. HINGWE and K. N. SUBRAMANIAN, *J. Mater. Sci.* **10** (1975) 183.
9. T. TAKASUGI, O. IZUMI and N. FAT-HALLA, *ibid.* **13** (1978) 2013.
10. T. TAKASUGI, N. FAT-HALLA and O. IZUMI, *Acta Metall.* **26** (1978) 1453.
11. N. FAT-HALLA, T. TAKASUGI and O. IZUMI, *J. Mater. Sci.* **14** (1979) 1651.
12. *Ibid, Met. Trans.* **10A** (1979) 1341.
13. T. TAKASUGI, N. FAT-HALLA and O. IZUMI, Proceedings of the 5th International Conference of the Strength of Metals and Alloys, Aachen, West Germany, August, 1979 (Pergamon Press, Oxford, (1979) p. 199.
14. N. FAT-HALLA, T. TAKASUGI and O. IZUMI, *Trans. JIM* **20** (1979) 1341.
15. T. TAKASUGI, N. FAT-HALLA and O. IZUMI, *J. Mater. Sci.* **15** (1980) 945.
16. T. E. MITCHELL and P. R. THORNTON, *Phil. Mag.* **8(2)** (1963) 1127.
17. R. E. JAMISON and F. A. SHERRILL, *Acta Metall.* **4** (1956) 197.
18. S. HANADA, M. MOHRI and O. IZUMI, *Trans. JIM* **16** (1975) 453.
19. T. YAMAGATA, H. YOSHIDA and Y. FUKUZAWA, *ibid.* **17** (1976) 393.
20. G. W. ARDLEY and A. H. COTTRELL, *Proc. Roy. Soc.* **A(219)** (1953) 328.
21. M. YAMAGUCHI and Y. UMAKOSHI, *Acta Metall.* **24** (1976) 1061.
22. M. AHLERS, R. PASCUAL, R. RAPACIOLI and W. ARNEODO, *Mater. Sci. Eng.* **27** (1977) 49.
23. G. J. SMITHELLES, "Metals Reference Book" 5th edition (Butterworths, London and Boston 1976) p. 975.
24. J. W. STEEDS, "Introduction to Anisotropic Elasticity Theory of Dislocations" (Clarendon Press, Oxford, 1973) p. 8.
25. J. A. RAYNE, *Phys. Rev.* **115** (1959) 63.
26. G. M. McMANUS, *ibid.* **129** (1963) 2004.

Received 27 March and accepted 1 May 1980.